Cold Regions Science and Technology 120 (2015) 197–204

Contents lists available at ScienceDirect

Cold Regions Science and Technology

journal homepage: www.elsevier.com/locate/coldregions

Mapping starting zone snow depth with a ground-based lidar to assist avalanche control and forecasting

Jeffrey S. Deems [a,*], Peter J. Gadomski [b], Dominic Vellone [c], Ryan Evanczyk [c], Adam L. LeWinter [b], Karl W. Birkeland [d], David C. Finnegan [b]

[a] National Snow and Ice Data Center, 449 UCB, University of Colorado, Boulder, CO 80309, USA
[b] US Army Corps of Engineers Cold Regions Research and Engineering Laboratory, 72 Lyme Rd., Hanover, NH 03755, USA
[c] Arapahoe Basin Ski Area, P.O. Box 5808, Dillon, CO 80435, USA
[d] USDA Forest Service National Avalanche Center, P.O. Box 130, Bozeman, MT 59771, USA

ARTICLE INFO

Article history:
Received 8 November 2014
Received in revised form 27 July 2015
Accepted 4 September 2015
Available online 9 September 2015

Keywords:
Spatial variability
Snow depth
Lidar
Avalanche
Avalanche control
Laser scanning

ABSTRACT

The distribution of snow depth in avalanche starting zones exerts a strong influence on avalanche potential and character. Extreme depth changes over short distances are common, especially in wind-affected, above-treeline environments. Snow depth also affects the ease of avalanche triggering. Experience shows that avalanche reduction efforts are often more successful when targeting shallow trigger point areas near deeper slabs with explosives or ski cutting. Our paper explores the use of high-resolution (cm scale) snow depth and snow depth change maps from terrestrial laser scanning (TLS) data to quantify loading patterns for use in both pre-control planning and in post-control assessment.

We present results from a pilot study in three study areas at the Arapahoe Basin ski area in Colorado, USA. A snow-free reference data set was collected in a summer TLS survey. Mapping multiple times during the snow season allowed us to produce time series maps of snow depth and snow depth change at high resolution to explore depth and slab thickness variations due to wind redistribution. We conducted surveys before and after loading events and control work, allowing the exploration of loading patterns, slab thickness, shot and ski cut locations, bed surfaces, entrainment, and avalanche characteristics. We also evaluate the state of TLS for use in operational avalanche control settings.

1. Introduction

The spatial distribution of snow depth in avalanche starting zones exerts a strong influence on avalanche formation and character (Schweizer et al., 2003, 2008). Extreme depth changes over short distances are common, especially in wind-affected, above-treeline environments. Snow depth affects snow density, hardness, and weak layer failure, and therefore the ease of avalanche triggering. Slab thickness and depth to weak layer affect the transmission of a triggering force (e.g. skier or explosives) to a buried weak layer — indeed avalanche control efforts at ski areas are often more successful when shallow trigger point areas next to deeper slabs can be targeted with explosives or ski cutting (Birkeland et al., 1995; Guy and Birkeland, 2013).

Knowledge of the spatial distribution of snow depth, and of differential loading due to precipitation or wind events, is valuable information to avalanche hazard assessment, control practitioners, as well as to backcountry travelers. Snow depth is typically measured manually by insertion of a ruled probe into the snowpack, or at in-situ stations via a sonic ranging instrument. Neither technique allows safe, repeat, non-destructive, and spatially-extensive sampling in avalanche starting zones.

In recent years Terrestrial Laser Scanners (TLS) have been used for mapping of snow depth and snow depth change (e.g. Deems et al., 2013; Egli et al., 2011; Grünewald et al., 2010; Prokop et al., 2008). In addition to the spatially-distributed, high resolution measurements, a sizable advantage of TLS over other methods is the ability to sample without exposing observers to avalanche hazard, and without disturbing the snow cover. Recent technological advances allow rapid data collection from multiple starting zones.

1.1. TLS measurement of snow depth

A TLS is an active remote sensing technology that uses laser pulses to measure range to target. By integrating positioning data (i.e. from GNSS or registration to existing survey data) the target ranges are converted into an x,y,z 'point cloud' of map coordinates and elevations. Subtraction of snow-free from snow-covered elevations provides a high-resolution (cm scale) map of snow depth, a data product which holds great

* Corresponding author.
E-mail address: deems@nsidc.org (J.S. Deems).

http://dx.doi.org/10.1016/j.coldregions.2015.09.002
0165-232X/

potential for monitoring snow accumulation patterns and operational assessment and planning of avalanche control efforts (Deems et al., 2013).

TLS survey methods have seen increasing use in snow depth mapping as equipment costs have decreased and the technology and processing software have become more available over the past decade. For example, Prokop (2008) conducted a thorough assessment of the suitability of TLS measurements for snow depth mapping, specifically in avalanche terrain. In subsequent studies, Prokop and colleagues evaluated new scanner capabilities (Prokop, 2009), investigated TLS methods for locating avalanche protection measures (Prokop and Delaney, 2012), integrated TLS measurements with avalanche dynamics models (Prokop et al., 2013a), and evaluated wind-drift modeling with TLS-derived snow maps (Prokop et al., 2013b), clearly demonstrating the applicability of TLS snow depth measurements and its wide range of potential applications. Grünewald et al. (2010) and Egli et al. (2011) conducted repeat TLS surveys during the melt season to evaluate spatial and temporal change in depth distributions. Maggioni et al. (2013) used combinations of TLS and airborne laser scanning to map snow depth pre- and post-avalanche control in their avalanche dynamics test site. These and other studies have clearly demonstrated that the high precision, high resolution elevation and snow depth data provided by TLS surveys enables a wide array of snow process and engineering studies.

Until recently, however, TLS surveys have either been limited to very short ranges due to the wavelength and power of the TLS system, or have required long-duration (often nighttime) data collection campaigns due to the slow speed of the scanner and limited detection capabilities at longer ranges. TLS technology developments have been improving both speed and range. For example, Prokop (2009) demonstrated measurement at ranges up to 1500 m with scan durations of approximately one hour, improving dramatically on prior survey constraints. The new Riegl VZ-4000 and VZ-6000 laser mapping systems allow similar or greater ranges, with faster data collection and higher resolution for mapping surface elevation of snow-free or snow-covered terrain. We have employed the Riegl VZ-4000 in snow-covered mountain environments and reliably retrieved ranges over 1000 m with 180° scan durations of 15–45 min (Fig. 1), with similar times and even longer ranges with the VZ-6000 (>5 km). This technology is a potentially revolutionary development for remote measurement of snow depth and depth change at high resolutions across complex terrain.

1.2. Pilot study, 2013–2014

The pilot study described here serves as a proof-of-concept for dataset production and for testing potential avenues for integration of the TLS products with ski area avalanche control operations. Survey scenarios were planned to test a range of operations support roles. Here we present highlights from the pilot study to assess the capability of TLS mapping in an operational avalanche control setting.

2. Methods

2.1. Field sites

We collected data during the summer (snow-off) and fall/winter (snow-on) of 2013/14 at Arapahoe Basin ski area in Colorado, (Fig. 2; Table 1). A-Basin is a high altitude, dry snow, continental environment, with extreme snow depth variability, extensive wind redistribution, and both storm snow and persistent weak layer driven avalanche problems.

The survey areas at A-Basin were chosen for safe access to scan positions and to represent a range of avalanche control problems. The East Wall, Montezuma Bowl, and the Steep Gullies areas represent a range of institutional experience: the East Wall (EW; 1.15 km^2) has been actively controlled since 1970, Montezuma Bowl (Z; 0.32 km^2) was part of a 2008 expansion and was the site of a post-control accident in 2013 (Greene and Brown, 2013), and the Steep Gullies (SG; 0.5 km^2) are a commonly-skied backcountry area that are part of a planned expansion. In combination, these areas present a range of aspects and slope angles for observing different loading and control events and testing the ability of the TLS system to map snow depth in complex terrain.

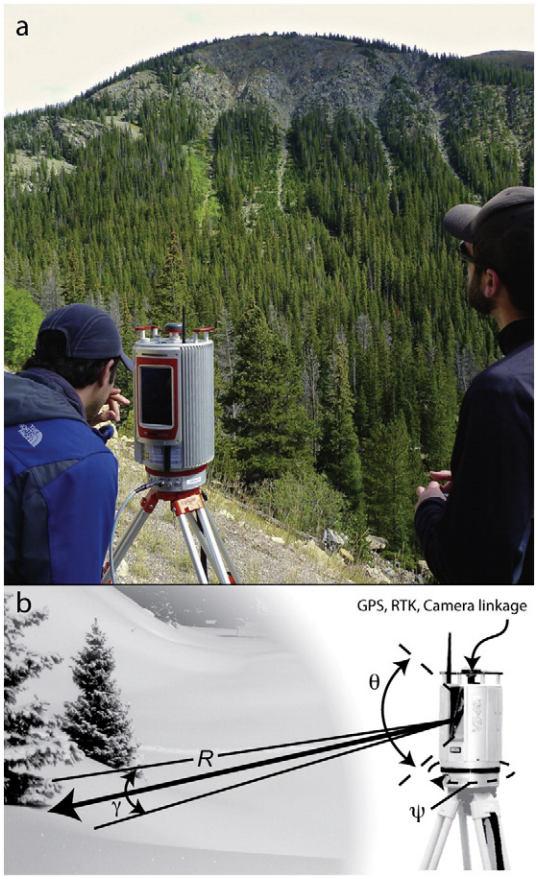

Fig. 1. (a) Riegl VZ-4000 at Steep Gullies scan site #1 during snow-free mapping; (b) schematic representation of scan parameters: range to target (R), beam divergence (γ), vertical angle range and resolution (θ), and horizontal angle range and resolution (ψ) (from Deems et al., 2013).

2.2. TLS scan parameters

The TLS system is deployed on a survey tripod, situated either on bare ground, stomped into the snowpack, or on infrastructure such as a gun mount or lodge deck, depending on conditions. We used two scan positions for each of the East Wall and Steep Gullies areas in order to provide multiple look angles on terrain features to minimize shadowing. The Montezuma terrain was observable from a single scan position. The snow-off scan was conducted using the VZ-4000, which operates at a wavelength of 1550 nm, where snow has relatively low reflectance (~10%) and rock/soil is much more reflective (~49%). We used the VZ-6000 for the initial 2 snow-on scans, which operates at a 1064 nm wavelength where snow is more reflective and allows for longer-range mapping. However, the 1064 nm wavelength is not inherently eye-safe, which limited our surveys to early morning hours prior to ski area opening. We used the VZ-4000 for subsequent surveys, which greatly relaxed the operational constraints while still providing ample range performance.

Scan parameters were chosen to maximize resolution (point density) over the target area, while minimizing collection time and post-processing steps (Table 2). Of interest is the pulse repetition

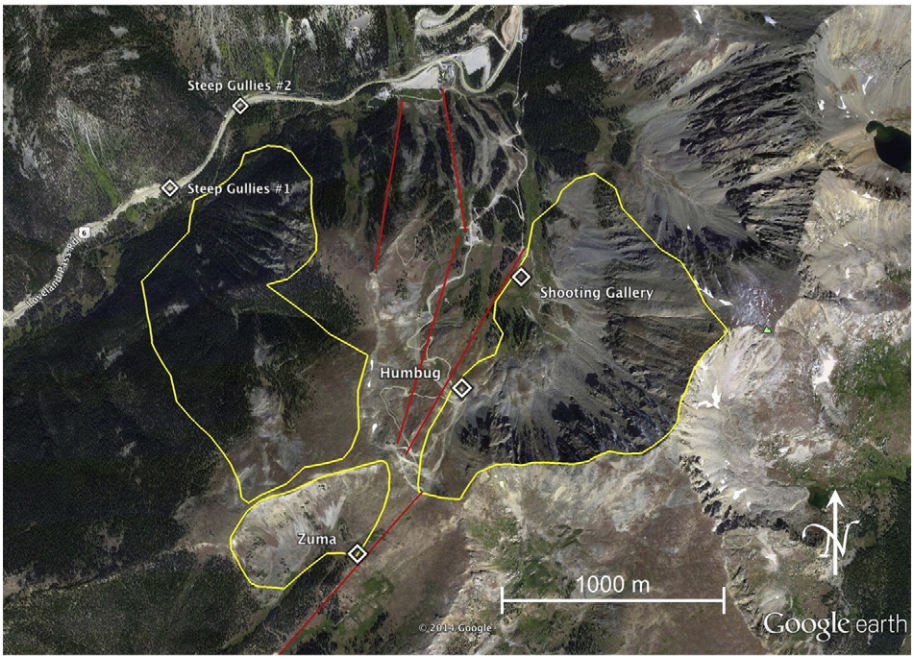

Fig. 2. Google Earth map view of the A-Basin ski area, Colorado, USA. TLS scan areas out-lined, with scan positions marked.

frequency (PRF). The TLS systems used are capable of PRF high enough to fire the next pulse before the prior pulse return has been detected, leading to range ambiguity and requiring manual assignment of points as a post-processing step (Deems et al., 2013). We chose the PRF such that minimal range ambiguity would occur.

2.3. Scan registration

Relative registration of scans is of paramount importance for accurate surface elevation differencing, and global registration is of lesser concern, though global registration (via GNSS positioning) can be used to achieve initial coarse registration (see §3.3). We did not use GNSS to geolocate our scan positions for coarse registration, but chose instead to manually designate several planar features in common between scans, usually exposed rock or permanent infrastructure. Coarse registration was then followed by semi-automatic fine registration using Riegl's Multi-Station Adjustment (MSA) algorithm (Riegl, 2015a; e.g. Prokop and Panholzer, 2009). We algorithmically identified snow-free planar regions in each of these scan areas – for the plane-finding algorithm, we manually configured the minimum and maximum plane dimensions, maximum plane error, and minimum number of points per plane – and ran the MSA tool to produce a three-dimensional, modified iterative least squares adjustment minimizing the RMSE difference between the two sets of planes.

Table 1
Snow-on scan dates, sites scanned, and weather since prior scan: T_{min}/T_{max}; storms and new snowfall; wind speed/direction.

Scan date	Scan sites	Weather history
12.19.2013	Z, EW, SG	−5/+5 °C, 1 period to −30 °C; 3 storms, 198 cm new snow; strong SW, W, NW
12.26.2013	Z, EW, SG	−18/−4 °C; 1 storm, 28 cm new snow; strong SW, NW
1.17.2014	Z, SG	−23/−2 °C; 4 storms, 132 cm new snow; strong W-NW
1.23.2014	Z, EW	−17/−0.5 °C; 0 new snow; moderate/strong NW
2.1.2014	Z, EW	−22/0.5 °C (1 h above 0 °C); 2 storms, 119 cm new snow; mod SW, strong W-NW
2.26.2014	Z, EW, SG	−22/−0.5 °C; 2 storms, 107 cm new snow; mod SW, strong WSW-NW
3.3.2014	Z, EW	−11/−1 °C; 1 storm, 45 cm new snow; strong NW–SW

2.4. Calculation of snow depth and snow depth change

The registered point clouds were rasterized to a 0.25 m grid, a resolution which minimized feature smoothing while remaining less sensitive to artifacts than a resolution closer to the nominal point spacing of 0.1 m. When the point spacing was larger than our grid size, e.g. in areas shadowed by rock outcrops, we used adaptive triangulation to fill the holes in the scan data. The vertical distance between the snow surface points and the reference surface (snow-off grid for snow depth, or prior snow surface grid for snow depth change) for each point was calculated for each point cloud data set.

2.5. Error assessment and sensor platform stability

An assessment of the error associated with the points collected by our TLS system requires accounting for multiple sources of error: errors inherent in the TLS platform (Schaer et al., 2007), errors induced by the interaction of the laser pulse with the target, errors associated with the scan data registration, and errors due to unstable scanner positions due to snow-on tripod setups. Additionally, smoothing due to interpolation used in snow depth calculation introduces additional error. The pilot nature of this project did not allow many resources for error quantification, so we rely on a qualitative examination to assess the reliability of our snow depth measurements.

A number of factors contribute to the point error introduced by the TLS system itself, a detailed discussion of which can be found in the literature, e.g. Morin (2002). Many laser scanner manufacturers, including Riegl, simplify these errors into a published accuracy and precision

Table 2
Typical TLS scan parameter values.

Parameter	Parameter range
PRF	50–150 kHz
Vertical angle increment	0.015°
Vertical angle range	60–120° from zenith
Horizontal angle increment	0.015°
Horizontal angle range	0–180°

value. Though these errors are given as constants but should in practice vary due to range and other factors, for the purposes of this study we accept the accuracy and precision values provided by the laser scanner manufacturer.

The geometry of a laser pulse introduces additional error into TLS measurements (Hartzell et al., in review; Glennie, 2007; Lichti and Gordon, 2004). A laser pulse has a finite beam width, leading to a potential discrepancy between the observed data point and the actual location of the surface that was measured by the beam. For example, using the published beam divergence for the VZ-4000 scanner (0.15 mrad) at 1000 m range produces a spot size of 15 cm on a beam-normal surface. On a surface with an incidence angle of 45°, the maximum range uncertainty due to beam divergence is 7.5 cm. Propagation of geometric error sources through the snow depth calculations results in depth errors of 5–15 mm (Hartzell et al., in review). In the study area terrain and scan locations, areas with strongly oblique incidence angles, and thus the highest vertical error component, are uncommon, and tend to occur near the edge of the scan areas where they are of lower concern.

An additional source of error in our point data is due to the mechanics of our scanner setup in the field. We conducted some of our scans, particularly those at the Montezuma Bowl site, with the scanner tripod legs buried in the snowpack. We did our best to provide a dense and stable base for the tripod, but data from the scanner's built-in inclination sensors reveal that the tripod did rotate during some scans (Fig. 3). The maximum amount of rotation was about 0.04° from the initial position, which translates to about 0.698 m of displacement in a point at 1000 m range. To correct for this change in the scanner orientation, we used the inclination sensor data (extracted via the Riegl RiVLib software library, Riegl Laser Measurement Systems, GmbH, 2015b) to calculate a moving average of the scanner rotation from its initial position and produce a time-variant estimate of the scanner orientation (Fig. 3). For each point in the point cloud, we constructed the rotation matrix of our time-variant estimate of the scanner's orientation at that point in time, and then applied the inverse of that rotation matrix to the coordinates of the lidar point. The end product was a point cloud that represented our best estimate of each point's position in the scanner's initial reference frame. We did not account for any translation in the scanner head, though the scanner probably both translated and rotated from its initial position due to snow compression under the tripod legs. This translation produces an additional undefined error source in our data, though practical estimates put this translation at less than one centimeter.

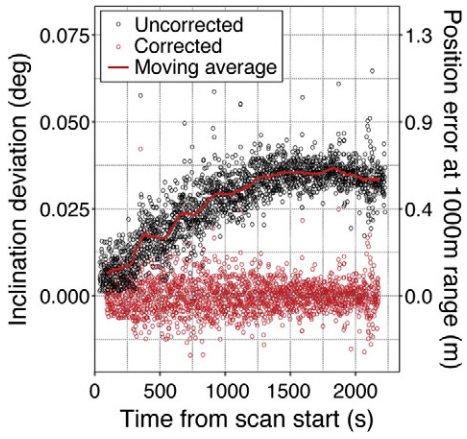

Fig. 3. Uncorrected (black dots), moving average (red line), and corrected (red dots) scanner inclination drift from a Montezuma Bowl scan on 3 March, 2014.

3. Results and discussion

The data collected allow an assessment of the utility of TLS-derived HS and dHS maps for various operational applications. The following discussion highlights notable results or opportunities from the 2013/14 pilot study.

3.1. Scan results and operational applications

3.1.1. Montezuma Bowl

Scan results from Montezuma Bowl on 17 and 23 January highlight the high resolution of the TLS measurement technique, as well as several potential applications and analyses (Figs. 4, 5).

Visible in the 17 January scan are two explosives-triggered avalanches, as well as numerous ski cuts and hand charge craters. The exceptional sensitivity of the TLS instrument is demonstrated by the detection of the traffic control rope line dividing the bowl, as well as around several other roped-off areas. Snow depth patterns show the importance of wind redistribution in this terrain (Fig. 4a).

The dHS map shows areas of accumulation and scour/ablation since the 26 December scan (Fig. 4b). Cross-loading and scour of terrain

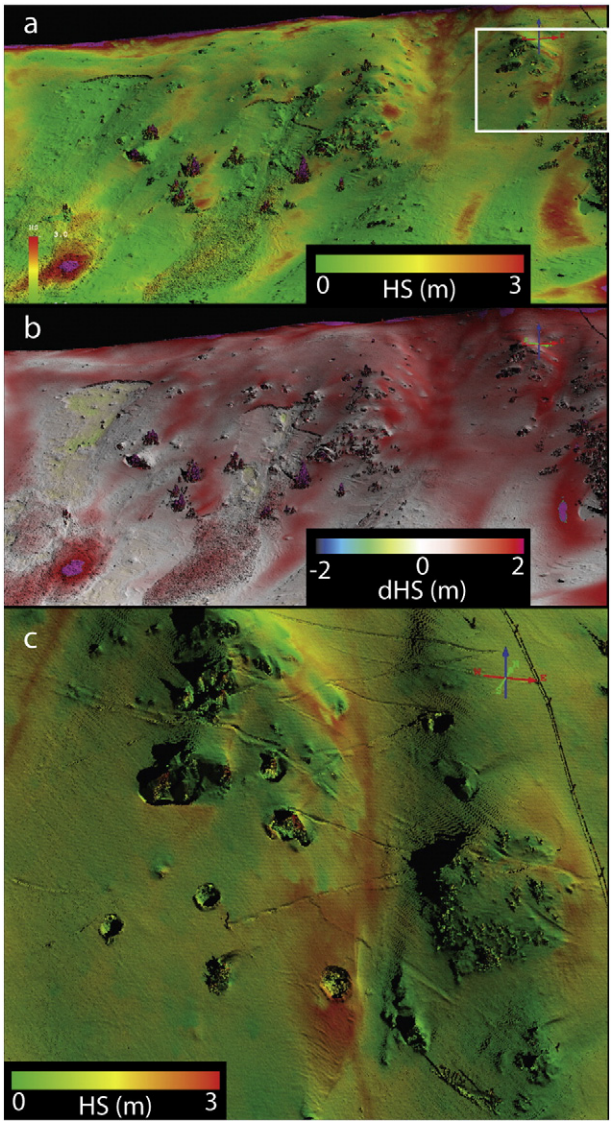

Fig. 4. Montezuma Bowl, 17 January, 2014. (a) HS; (b) dHS relative to 26 December; (c) HS subset showing ski cuts and hand charge craters near a deep snow pocket.

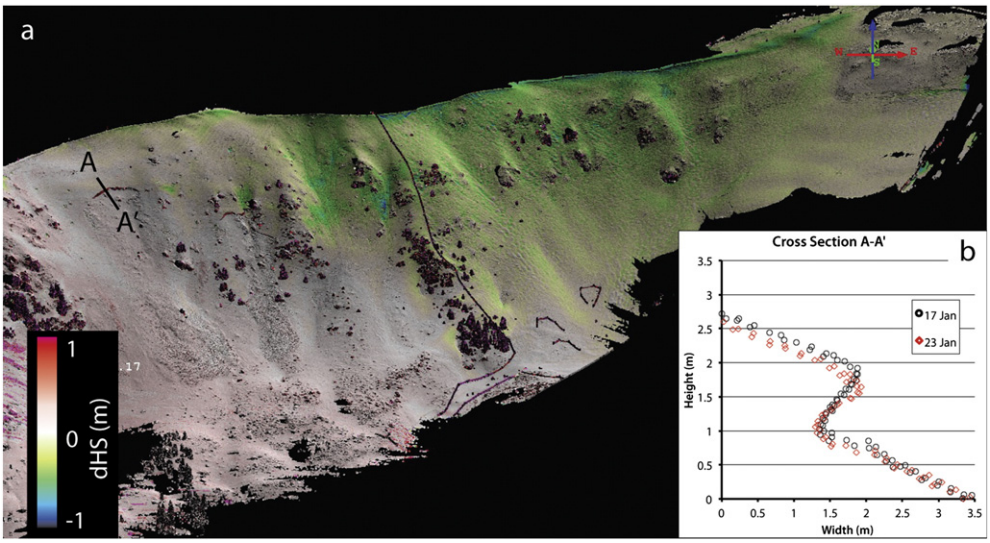

Fig. 5. Montezuma Bowl, 23 January, 2014. (a) dHS illustrating skier compaction and snowmelt; (b) cross section along A-A′, showing surfaces from 17 and 23 January and settlement plus creep and/or wind drifting over that time period.

features from southwest winds are quite evident, and cornice growth can be seen all along the ridge, with increases of greater than 2 m in the northern half due to loading from northwesterly winds. One slab avalanche occurred in a loaded terrain pocket at a break in slope, as is common, but the complex loading pattern around the crown suggests that slab variability or continuity limited propagation extent. The second fracture line connects rocks, trees, and shallow areas, and the bed surface shows evidence of scour and/or downstepping of the slab failure into lower layers.

Closer to the rope line is a loaded gully with one particularly deep pocket that would certainly warrant caution and control attention (Fig. 4c). Ski cuts and hand charge craters are readily seen on the deep pocket, as well as in the shallow areas surrounding it, suggesting that the control efforts have soundly tested the local stability, targeting deep and shallow areas as well as rock outcrops and terrain convexities. This instance illustrates the potential application of the TLS system for post-control assessment, providing a means to evaluate control results and the size of any remaining hangfire, as well as to examine potential reasons for non-results, e.g. disconnected slabs or shots placed in locations with deep accumulation. The TLS maps could also be used to digitize shot placement and ski cut locations to populate digital avalanche control records.

The 23 January dHS map shows mostly depth reduction since 17 January, with several interesting patterns. The southwest end of the bowl (Fig. 5a, left part of image) indicates minor accumulation, while the northeast half shows pronounced depth decreases; northeast of the control rope line, the mogul pattern indicates that the 0.2–0.5 m depth decrease is due primarily to skier compaction. The capability of the TLS system to quantify and map skier compaction could be applied in an operational context to estimate areas in which the compaction is affecting a weak or slab layer of concern.

Substantial depth decreases are also seen south of the rope line, but this area was closed to public skier traffic. Field observations on 23 January note widespread explosives residue on the snow surface in these areas, as well as abundant surface runnels from snowmelt, despite subfreezing air temperatures during this period. Clearly, the reduced snow surface albedo from the blast residue in combination with the southerly exposure of the terrain allowed strong surface melt and depth reduction. Though the TLS dHS map cannot reveal the depth of liquid water penetration, or which snow layers were reduced in thickness, coincident manual measurements could be collected to estimate the impacts of the surface melt over the full starting zone.

Cross-sections through the southernmost avalanche crown from 17 to 23 January reveal settlement and either creep effects or snow drift accumulation on the crown face (Fig. 5b). Settlement of the relatively undisturbed snow above the crown measures about 10 cm, while below the crown very little settlement is observed, likely due to compaction of the bed surface during the avalanche event. The surrounding area shows 0–10 cm of accumulation, suggesting that the actual settlement was greater than 10 cm and was offset by drifting snow. The crown face itself has tipped or grown downhill, with increased downslope displacement at the top of the crown, consistent with either differential creep rates (e.g. McClung and Schaerer, 2006) or with drifting snow accumulating on the crown edge as with cornice growth.

3.1.2. East Wall

We collected two East Wall scans on 1 February, pre- and post-control operations, and the two dHS maps reveal numerous slab and avalanche release features, and suggest several applications (Fig. 6). The most extensive avalanche in the dataset was released with a single avalauncher shot (shot location marked with "X"). The white coloration in the bed surface indicates that the slide ran on the old snow surface (white indicating 0.0 m dHS since 23 Jan). Green and blue colors show areas where the avalanche scoured into the old snow, and occur primarily within gully features and areas of flow convergence.

Several portions of stauchwall are readily observed, and offer the potential for measurement of slab volume, which has been shown to be useful for calibration or verification of dynamics models (e.g. Prokop et al., 2015; Prokop and Delaney, 2010). For example, a rough slab delineation using crown, flank, stauchwall, and flow divides (Fig. 6, area "A") from the post-control data set and applied to the slab area to the pre-control dHS map produces a slab volume of 5840 m^3. We calculate the volume of the corresponding debris pile to be 2980 m^3. Assuming an average slab density of 200 kg/m^{-3}, the mass of slab and debris balance if the debris density is about 390 kg/m^{-3}, which is within the typical debris density range (McClung and Schaerer, 2006). Of course, this simplistic treatment considers neither entrainment (scour is evident in the dHS map) nor compaction of the existing snow below the debris, but it is clear that, when combined with field measurements, TLS holds promise as a model validation data source.

3.1.3. Steep Gullies

The complex terrain in the Steep Gullies area presents numerous scanning and processing challenges. The scan positions were set on

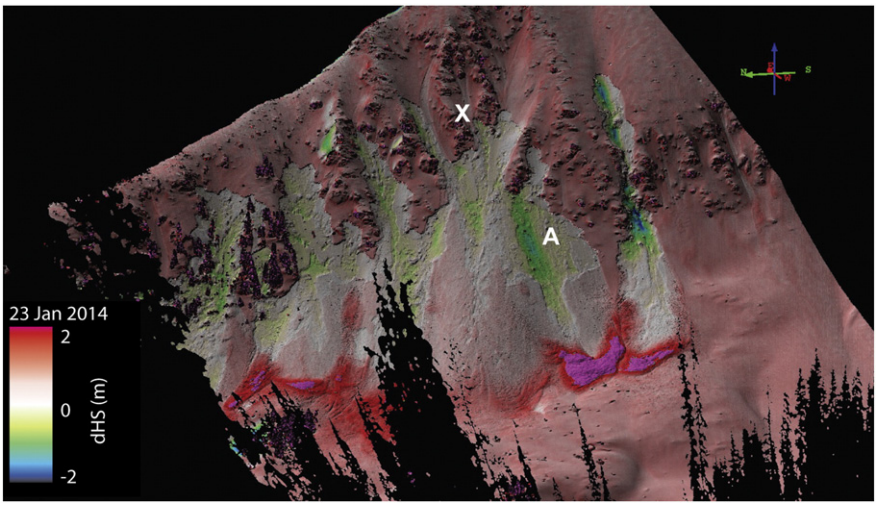

Fig. 6. East Wall on 1 February, 2014. dHS relative to 23 January. Large to left avalanche was initiated by a single avalauncher round at point "X". Slab volume calculated for area around "A".

the highway shoulder, and were deemed too dangerous to occupy in unplowed conditions. There are very few planar features in the terrain, which complicates feature mapping and data set registration. However, we successfully collected several scans, which reveal snow loading patterns and avalanche character in this unmanaged, "sidecountry" terrain.

Fig. 7a shows a portion of this complex terrain, with several notable drift accumulation areas. As expansion plans proceed, the TLS data could prove valuable for characterizing accumulation patterns that occur under certain storm/wind directions, for use in snow safety plan development and for planning placement of explosives delivery trams. In particular, combined TLS mapping of accumulation patterns and a wind redistribution model could be an effective application for characterization and exploration of slab distributions under various meteorologic conditions (e.g. Prokop et al., 2013a, 2013b; Prokop, 2008). The skier-triggered avalanche in Fig. 7b consists of several disconnected slab pockets and illustrates the terrain management challenges in this area.

3.2. Error assessment and TLS survey techniques

3.2.1. Snow pit depth comparison

The scope of this pilot study did not allow for a coordinated manual validation of snow depth calculations, however one scan date in Montezuma Bowl coincided with excavation of a snow pit and measurement of snow properties by Arapahoe Basin snow safety personnel. The extent of this snow pit was quite evident in the scan data (not shown), and thus it was possible to query TLS point snow depth values near the corner of the snow pit where depth was manually recorded. The TLS and manual depths in this location agreed to within one centimeter. While this is by no means a comprehensive validation, it is an encouraging result.

3.2.2. Scan registration

The MSA procedure was used iteratively to minimize the error between snow-free planar features in common to both of the data sets being registered, and the MSA tool produces general and spatial statistics about the distribution of these errors. RMSE values for the final MSA adjustments were between 2 and 5 cm for both Zuma and East Wall sites. Errors were generally normally distributed, and spatial analysis indicated that the scan adjustments were evenly spread throughout the scan area, indicating that no particular spatial or statistical bias was present.

3.2.3. Gridding

In order to calculate HS and dHS from the point cloud data, we gridded the reference dataset on a 0.25 m grid. This grid size is larger than the data point spacing would support throughout our scan regions, but was chosen as a balance between highest resolution and the need to

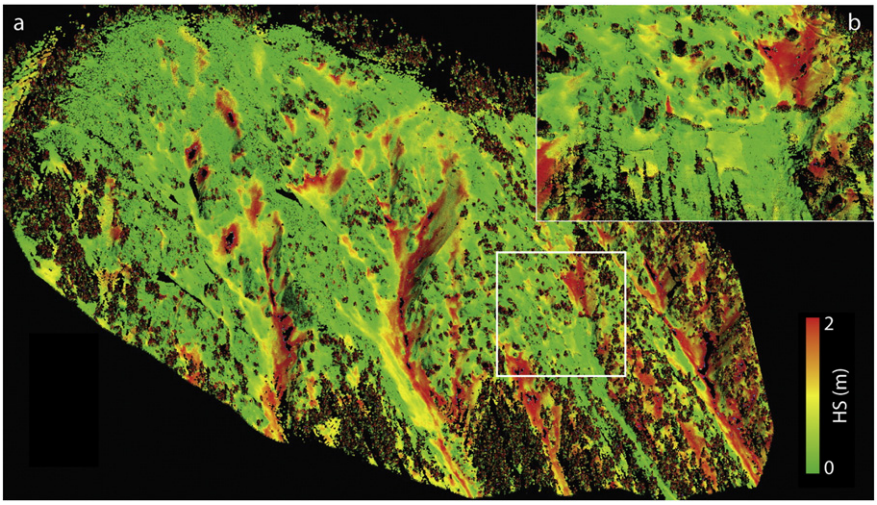

Fig. 7. Steep Gullies on 17 January, 2014. (a) HS; (b) subset showing skier-triggered avalanche.

interpolate areas with partial shadowing. The choice of gridding algorithm can influence the amount of smoothing and thus the calculated vertical displacement, especially in areas with sparse data points (e.g. at long range) or complete lack of data points (e.g. in shadows). The gridding step smooths the reference surface compared to the point cloud, but has the additional benefit of reducing the effect of any erroneous points that survived filtering and data set QC. Since our scan positions were relatively constant throughout the season, the areas of low or no data were relatively constant from scan to scan, and as a result relatively few HS and dHS values used triangulated grid data; the vast majority of HS and dHS values were calculated using a grid value averaged from several point measurements. Changes to the gridding extrapolation method would therefore only affect edge cases, such as at the edge of data shadows or in overhanging areas such as cliffs.

3.3. Recommended improvements to TLS survey procedures

For change detection or differential volume change calculations using multiple lidar data sets, relative scan registration is the most critical element. In rough terrain, where large changes in elevation can occur over extremely short horizontal distances, small registration offsets can produce large errors in the final difference product. Absolute (geographic) registration is of secondary importance, and is primarily of interest for integration with ancillary data sets for visualization. However, absolute registration can provide a reasonably efficient pathway to achieve relative registration in certain circumstances.

To achieve relative registration, two steps are commonly employed in sequence: an initial coarse registration is followed by a more detailed and robust fine registration. Coarse registration can be achieved by setting up instrumentation over known points, employing permanent infrastructure (specifically scanner mounts and reflector targets), via high-accuracy GNSS surveys, or by manually identifying target features in common between scans and adjusting the scans such that the features roughly match. When collecting scan data for this pilot study, we chose data collection procedures with an eye towards minimizing scan time and equipment requirements, as well as minimizing infrastructure impacts on the Arapahoe Basin ski area — we opted to forego permanent installations and GNSS surveys and rely on manual feature matching for coarse registration.

Coarse registration is then followed by a more robust, statistically based fine registration. Fine registration methods are commonly based on an iterative-closest-point (ICP) matching algorithm. As described above, we used the Riegl MSA algorithm in this application.

Data collection time and processing time could also be reduced by creating a permanent fixed mount for the TLS instrument at a scan location. This mount would be surveyed with high-precision GNSS after installation, and at least one cylindrical reflector would be installed and surveyed near the scanner mount. This procedure would allow data collection and coarse registration without high-precision GNSS, since the locations of the scanner and the reflector are known a-priori, and would obviate issues due to the scanner tripod shifting when erected on snow (see §2.5 above). This procedure has the highest infrastructure impact, but requires the least amount of work to collect and register each scan — coarse registration would be achieved implicitly and processing would proceed directly to fine registration. Several combinations of permanent infrastructure and GNSS surveys are possible for increased survey and data production efficiency, with the optimal choice for a given project depending on survey area characteristics, access, and the availability of GNSS survey equipment.

3.4. Conclusions and future work

Our results provide exciting insights into snow accumulation and avalanche processes, as well as for the potential for informing and supplementing operational avalanche control efforts. We have identified several promising avenues for future development and application, and identified pathways for integration of the TLS data products in an operational setting.

The principal challenge for operational use of TLS snow depth maps is the timely generation of data products. As such, minimizing data collection and processing time while maintaining accuracy is of great interest. Our experience on other projects suggests that a high accuracy (static or post-processed kinematic) GNSS survey of scan locations can provide sufficient accuracy to achieve coarse registration, reducing post-processing effort. However the GNSS survey adds time and complexity to the data collection effort, and unless global registration is ultimately required, the GNSS survey effort may offset the post-processing time savings achieved. Equivalent post-processing and scan registration savings can be achieved via installation of permanent scanner mounts and reflectors. Re-occupation of a permanent mount minimizes scan location uncertainty, and at least one reflector tie point which remains unchanged throughout the season would eliminate the need to manually identify identical features in common between scans. Either the GNSS survey or reoccupation of permanent sites can eliminate the need for the coarse registration step and would thus help enable rapid turnaround data products for best operational relevance.

The other primary challenge for operational integration is the type of final data products. Static images of colored point clouds (such as those in this document) provide a sense of the detail captured in the TLS products, but much greater value can be achieved through direct interaction with a 3D dataset. Enabling this interaction is a key challenge for integration with avalanche control operations — ideally data products can be provided without the need for acquisition of or experience with specialized software packages. Our initial efforts suggest that export of images to Google Earth meets several of these goals, but suffers from loss of resolution and detail. Recently released web browser-based point cloud visualization tools offer a potential solution. Integration of products with existing digital avalanche atlases would be useful for control route planning and event documentation.

Different information is contained in the HS and dHS data products. For operational interests where new slab or storm snow distributions are of primary concern, it is likely that the dHS products would be of most utility, especially if scans can be collected prior to and following a precipitation or wind event. In such a case, it is likely that the dHS map can safely be assumed to represent the distribution of new slab thickness across the domain. Quantification of loading patterns could also be useful for comparison with experiential knowledge possessed by individuals with a history of conducting avalanche assessment in the area of operation, and for identifying unusual loading patterns that do not fit with conventional wisdom.

Maps of HS are likely most useful for identifying threshold depths, e.g. for identifying areas susceptible to high temperature gradients and facet or depth hoar development. Snow depth maps can also be useful for relating manual measurements (of stratigraphy, depth, etc.) to the wider terrain, or conversely for identification of preferred manual measurement locations.

It is difficult to overstate how visually compelling the TLS HS and dHS maps can be. As such, education, public outreach, and marketing opportunities should not be overlooked. In particular, quantification and visualization of complex snow accumulation patterns would be of direct benefit to avalanche education, particularly at higher levels that deal directly with issues pertaining to spatial variation in snow properties.

In addition to refinement and further deployment of the ski area operational support explored in this pilot study, expansion of the TLS mapping techniques to highway control operations would be a natural next step. Assessment and verification of control results would add useful quantitative decision-support data and be a valuable tool in maintaining highway corridor safety. Quantification of slab and debris volumes provides a highly accurate data source for integration with avalanche dynamics models (e.g. Prokop et al., 2015). Additionally,

our team is developing an autonomous TLS system, meant to constantly monitor and transmit data products from remote locations (LeWinter et al., 2014).

TLS technology has advanced rapidly in recent years, and the latest generation of sensor systems has enabled the starting zone mapping described here on time scales relevant for operational interests. As the TLS technology becomes more widely available and at lower cost, the future for avalanche research and application using this powerful tool holds much promise.

Acknowledgments

We would like to acknowledge the Arapahoe Basin ski patrol, mountain operations, and management for enabling the data collection and collaborating towards operational integration. We are also grateful to Riegl Laser Measurement Systems GmbH for their innovation and leadership — their new long-range TLS systems make this project possible. Thanks to our two reviewers, whose comments and suggestions greatly improved this manuscript. This work was partially supported by a CIRES Innovative Research Grant, and by a Theo Meiners Research Grant from the American Avalanche Association — we are indebted to Theo for his energy and inspiration to incorporate new science and tools into operational avalanche decision-making.

References

Birkeland, K.W., Hansen, K.J., Brown, R.L., 1995. The spatial variability of snow resistance on potential avalanche slopes. J. Glaciol. 41, 183–189.

Deems, J.S., Painter, T.H., Finnegan, D.C., 2013. Lidar measurement of snow depth: a review. J. Glaciol. 59, 467–479. http://dx.doi.org/10.3189/2013JoG12J154.

Egli, L., Jonas, T., Grünewald, T., Schirmer, M., Burlando, P., 2011. Dynamics of snow ablation in a small Alpine catchment observed by repeated terrestrial laser scans. Hydrol. Process. 26, 1574–1585. http://dx.doi.org/10.1002/hyp.8244.

Glennie, C., 2007. Rigorous 3D error analysis of kinematic scanning LIDAR systems. J. Appl. Geodesy 1 (3).

Grünewald, T., Schirmer, M., Mott, R., Lehning, M., 2010. Spatial and temporal variability of snow depth and ablation rates in a small mountain catchment. Cryosphere 4, 215–225. http://dx.doi.org/10.5194/tc-4-215-2010.

Guy, Z.M., Birkeland, K.W., 2013. Relating complex terrain to potential avalanche trigger locations. Cold Reg. Sci. Technol. 86, 1–13. http://dx.doi.org/10.1016/j.coldregions.2012.10.008.

Hartzell, P.J., Gadomski, P.J., Glennie, C.L., Finnegan, D.C., Deems, J.S., 2015w. Rigorous error propagation for terrestrial laser scanning with application to snow volume uncertainty. J. Glaciol. (in review).

LeWinter, A.L., Finnegan, D.C., Hamilton, G.S., Stearns, L.A., Gadomski, P.J., 2014. Continuous monitoring of Greenland outlet glaciers using an autonomous terrestrial LiDAR scanning system. Design, Development and Testing at Helheim Glacier, Abstract 17768, American Geophysical Union 2014 Fall Meeting, San Francisco, CA, pp. 15–19 (Dec.).

Lichti, D., Gordon, S., 2004. Error propagation in directly georeferenced terrestrial laser scanner point clouds for cultural heritage recording. Proc. of FIG Working Week, Athens, Greece, pp. 1–16 (May).

Maggioni, M., Freppaz, M., Ceaglio, E., Godone, D., Viglietti, D., Zanini, E., Barbero, M., Barpi, F., Brunetto, M.B., Bovet, E., Chiaia, B., De Biagi, V., Frigo, B., Pallara, O., 2013. A new experimental snow avalanche test site at Seehore peak in Aosta Valley (NW Italian Alps)—part I: conception and logistics. Cold Reg. Sci. Technol. 85, 175–182. http://dx.doi.org/10.1016/j.coldregions.2012.09.006.

McClung, D.M., Schaerer, P.A., 2006. The Avalanche Handbook. 3rd ed. The Mountaineers (347 pp.).

Morin, K.W.K., 2002. Calibration of Airborne Laser Scanners. 20179. University of Calgary, Calgary, Canada, p. 134.

Prokop, A., 2008. Combining wind field modeling with spatial snow depth measurements for avalanche forecast purpose. *Proceedings International Snow Science Workshop, Whistler, BC, Canada*, pp. 674–678.

Prokop, A., 2009. Terrestrial laser scanning for snow depth observations: an update on technical developments and applications. *Proceedings of the International Snow Science Workshop, Davos*, pp. 192–196.

Prokop, A., Delaney, C., 2010. A high resolution approach to defining spatial snow height distribution in avalanche release zones for dynamic avalanche modeling. *Proceedings International Snow Science Workshop, Squaw Valley*, CA, USA, p. 2010.

Prokop, A., Delaney, C.M., 2012. Positioning of avalanche protection measures using snow depth mapping via terrestrial laser scanning. *Proceedings International Snow Science Workshop, Anchorage, AK USA*, pp. 983–988.

Prokop, A., Panholzer, H., 2009. Assessing the capability of terrestrial laser scanning for monitoring slow moving landslides. Nat. Hazards Earth Syst. Sci. 9 (6), 1921–1928.

Prokop, A., Schirmer, M., Rub, M., Lehning, M., Stocker, M., 2008. A comparison of measurement methods: terrestrial laser scanning, tachymetry and snow probing for the determination of the spatial snow-depth distribution on slopes. Ann. Glaciol. 49, 210–216.

Prokop, A., Schön, P., Singer, F., Pulfer, G., Thibert, E., 2013a. Determining avalanche modelling input parameters using terrestrial laser scanning technology. Proceedings International Snow Science Workshop, Grenoble – Chamonix Mont-Blanc, France, pp. 770–774.

Prokop, A., Schön, P., Vionnet, V., Naaim-bouvet, F., Guyomarc, G., Durand, Y., Bellot, H., Singer, F., Nishimura, K., 2013b. A comparison of terrain-based parameter, wind-field modelling and TLS snow depth data for snow drift modelling. *Proceedings International Snow Science Workshop, Grenoble – Chamonix Mont-Blanc, France*, pp. 108–113.

Prokop, A., Schön, P., Singer, F., Pulfer, G., Naaim, M., Thibert, E., Soruco, A., 2015. Merging terrestrial laser scanning technology with photogrammetric and total station data for the determination of avalanche modeling parameters. Cold Reg. Sci. Technol. 110 (2015), 223–230.

Riegl Laser Measurement Systems, GmbH, 2015a. RiVLib. http://www.riegl.com/index.php?id=224 (accessed June 6, 2015).

Riegl Laser Measurement Systems, GmbH, 2015b. RiSCAN Pro. http://www.riegl.com/products/software-packages/riscan-pro/ (accessed June 6, 2015).

Schaer, P., Skaloud, J., Landtwing, S., Legat, K., 2007. Accuracy estimation for laser point cloud including scanning geometry. 5th International Symposium on Mobile.

Schweizer, J., Jamieson, B., Schneebeli, M., 2003. Snow avalanche formation. Rev. Geophys. 41, 1016–1041.

Schweizer, J., Kronholm, K., Jamieson, J., Birkeland, K., 2008. Review of spatial variability of snowpack properties and its importance for avalanche formation. Cold Reg. Sci. Technol. 51, 253–272.